Innovative Food Science and Emerging Technologies 61 (2020) 102312

Contents lists available at ScienceDirect

Innovative Food Science and Emerging Technologies

journal homepage: www.elsevier.com/locate/ifset

Flux evaluation based on fouling mechanism in acoustic field-assisted ultrafiltration for cold sterilization of tender coconut water

Archana G. Lamdande[1], Rochak Mittal, Raghavarao K.S.M.S.*

Academy of Scientific and Innovative Research, New Delhi, India
Department of Food Engineering, CSIR-Central Food Technological Research Institute (CFTRI), Mysuru 570 020, India

ARTICLE INFO

Keywords:
Food processing
Ultrafiltration
Acoustic field
Enzyme activity
Fouling mechanism

ABSTRACT

Membrane-based processing was attempted as a clean, green and energy-efficient method for cold sterilization of tender coconut water (TCW). Ultrafiltration of TCW was carried out at four different pressures employing two different polyethersulfone membranes, using a stirred cell. Permeate flux was evaluated based on different fouling mechanisms which are analysed employing Hermia's model. The objective of the study was to examine the efficacy of ultrafiltration for cold sterilization of TCW while retaining good sensory quality. The effect of acoustic field (ultrasonication) on the performance of ultrafiltration has been evaluated. Permeate flux increased on the application of ultrasonication. Enzyme activities in TCW permeate were found to reduce after ultrafiltration with good sensorial acceptability. Microbial load of TCW after ultrafiltration was observed to decrease from 4.16 to 0.0 log CFU/mL, achieving cold sterilization. Sensorial quality of ultrafiltered TCW was found to be good after three months storage period with zero microbial count.

1. Introduction

Tender coconut water (TCW) is a natural and ideal rehydrating drink due to its mineral composition, sugar content and micronutrients such as vitamins and inorganic ions. It is popular as a sports drink and gained attention as a natural functional drink (Prades, Dornier, Diop, & Pain, 2012). Tender coconuts can be kept at ambient conditions up to 15 days after plucking from a tree. However, TCW exhibits a change in colour on its exposure to the environment due to oxidation of naturally presented enzymes, namely polyphenol oxidase and peroxidase (Matsui, Gut, De Oliveira, & Tadini, 2008). The sensorial and nutritional qualities of TCW can also be affected by these enzymatic reactions. Microbial contamination in TCW collected by traditional techniques would be in the order of 10^6 per mL, making it unsuitable for consumption (Reddy, Das, & Das, 2005).

TCW is termed as “miracle water” for its various health benefits. It contains around 95.5% water, 0.1% fat, 4% carbohydrates, 0.02% calcium, 0. 01% phosphorous, 0.5% iron with some of the amino acids, B complex vitamins, vitamin C and mineral salts (Tan, Cheng, Bhat, Rusul, & Easa, 2014; Vigliar, Sdepanian, & Fagundes-Neto, 2006; Yong, Ge, Ng, & Tan, 2009).

Traditionally, coconut water is marketed in the nut itself, which involves transportation problems, perishability and storage-related issues. Therefore the demand for processed TCW is increasing (Magalhães, Gomes, Modesta, Matta, & Cabral, 2005). The coconut water (after opening the nut), may get spoiled due to exposure to the environment and unhygienic practices of handling (human contact). Hence, proper technology development is necessary to reduce contamination and spoilage while retaining the sensory qualities. Existing technologies are based on the addition of antimicrobial agents and thermal processing for shelf life extension and enzyme inactivation, which cause changes in delicate flavour and loss of nutrients of fresh TCW (Campos, Souza, Coelho, & Gloria, 1996; Chowdhury, Aziz, & Uddin, 2005). There is ample scope for alternate methods devoid of thermal treatment and addition of external agents. Membrane processing is certainly one such method. Membrane processing due to its low energy requirements and low carbon footprint has gained popularity in recent times. The major applications of membrane processing include clarification and concentration of fruit juices, whey etc. (Baldasso, Barros, & Tessaro, 2011; Cassano, Marchio, & Drioli, 2007). Due to the non-thermal nature of membrane processing (microfiltration and ultrafiltration), it can be carried out at room temperature without much loss in original quality. Ultrafiltration is reported as a green technique for various liquid food commodities, for example, whey solution (Corbatón-Báguena, Álvarez-Blanco, & Vincent-Vela, 2018).

Both microfiltration and ultrafiltration are pressure-driven

* Corresponding author.
E-mail addresses: lamdandaag@uasd.in (A.G. Lamdande), raghavarao@cftri.res.in (R. K.S.M.S.).
[1] Current address: Department of Food Processing and Technology, College of Community Science, University of Agricultural Sciences, Dharwad 580005, India.

https://doi.org/10.1016/j.ifset.2020.102312
Received 24 May 2019; Received in revised form 15 January 2020; Accepted 5 February 2020
Available online 06 February 2020

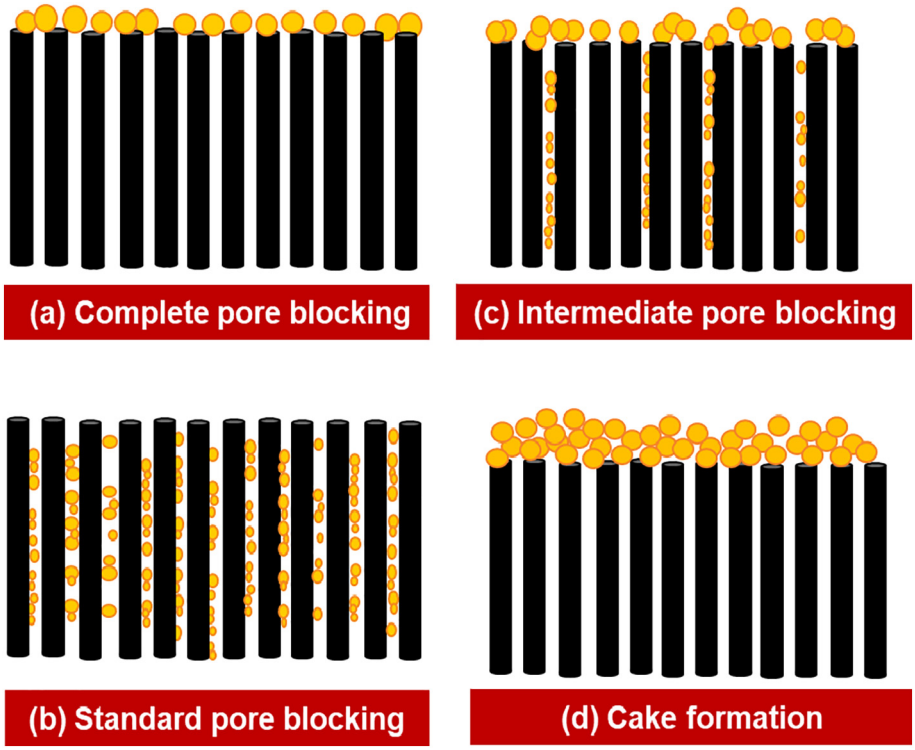

Fig. 1. Schematic representation of membrane subjected to different types of membrane fouling (a) Complete pore-blocking, (b) Standard pore-blocking, (c) Intermediate pore-blocking and (d) Cake formation.

processes that achieve separation based on size. Several reports on microfiltration of TCW (employing conical flask set-up) are available, whereas, only a few reports on the ultrafiltration of TCW are available (employing stirred cell). Membrane fouling and concentration polarisation due to rejection of suspended solids (present in the feed) at the membrane surface are the main issues during ultrafiltration which reduce the permeate flux, in turn, decreasing the processing performance (Saha, Balakrishnan, & Ulbricht, 2009). Membrane fouling may occur either by particle deposition on the membrane surface or inside the membrane pores or due to a combination of both (Maruyama, Katoh, Nakajima, & Nabetani, 2001; Wang, Wang, & Fukushi, 2008). It was reported that the extent of fouling depends strongly on the properties of the feed solution, membrane material and operating conditions (Babu & Gaikar, 2001). There are various types of fouling mechanisms reported, which can be described by blocking filtration laws, namely complete blocking, standard pore blocking, intermediate pore blocking and cake formation. These fouling mechanisms were first proposed by Hermia and thus, known as Hermia's model (Hermia, 1982). Hermia's model has been used to evaluate the nature of fouling occurred during clarification of red plum juice (Nourbakhsh, Emam-Djomeh, Mirsaeedghazi, Omid, & Moieni, 2014), filtration of protein, polysaccharide solutions (Palacio, Ho, & Zydney, 2002) and polysaccharide macromolecules (Sarkar, 2013). Hence, proper analysis and understanding of these membrane fouling mechanisms are essential to minimize fouling in order to improve the performance of ultrafiltration. Membrane fouling and concentration polarisation can be reduced significantly by the application of the acoustic field. Ultrasonication has been reported to result in a significant enhancement in transmembrane flux during membrane processing of various feed materials such as whey, milk etc. (Latt & Kobayashi, 2006; Muthukumaran et al., 2004). Ultrasonication creates cavitation in the liquid medium and near the membrane surface that is capable of dislodging the concentration polarisation layer and removes the particles from the membrane surface (Jin et al., 2014; Juang & Lin, 2004; Narayan et al., 2002). Cavitation consists of rarefaction and a compression cycle, which leads to the formation, growth and collapse of microbubbles, disturbing the fouling layer and causing cleaning of the membrane (Simon, Penpenic, Gondrexon, Taha, & Dorange, 2000).

Different mechanisms such as complete pore blocking, intermediate pore blocking, standard pore blocking, and cake formation are not reported in the earlier reports available on the ultrafiltration of tender coconut water except the recent work by Karmakar and De, where resistance in the series model was employed (Karmakar & De, 2017).

In general, the degree of membrane fouling (adsorption, pore blockage and formation of cake layer) increases with the complexity of the feed composition, processing conditions and membrane properties. However, the predominant fouling mechanism occurring during membrane processing (ultrafiltration) can be detected by evaluating the fouling mechanisms.

In the present study, polyethersulfone (PES) membranes of different molecular weight cut-off (30 and 100 kDa) were used for the ultrafiltration of TCW. Different mechanisms were employed to evaluate the prominent fouling that occurred during ultrafiltration of TCW. Only a few reports are available on the ultrafiltration of TCW. Whereas, practically no reports are available on acoustic field-assisted ultrafiltration of TCW.

The objective of the present work is to develop an ultrasound-assisted membrane-based method for achieving the cold sterilization of TCW. Both being non-thermal processes can retain the nutritional, chemical, and organoleptic properties of TCW. Accordingly, the process parameters such as molecular weight cut off and transmembrane pressure were standardized.

2. Theoretical aspects

In order to get a comprehensive picture of the theoretical analysis of the membrane filtration process, we shall examine the theoretical models, the assumptions and the associated physical picture of the process besides the inferences drawn (Bowen, Calvo, & Hernandez, 1995; Gonsalves, 1950).

Let us consider the unit operation of filtration employing a membrane or filter medium having a large number of pores as schematically presented in Fig. 1 (i) Straight pore.

It is assumed that (1) The pores are cylindrical in shape and run parallel to each other across the thickness of the membrane, (2) All the pores have same diameter and length (3) the fluid flow is perpendicular to the membrane surface (a valid assumption in case of the stirred cell).

The fluid (slurry/solution) that is being filtered has suspended particles/soluble solutes at a concentration of C_p (#/m^3) out of which C_p' particles will block the pores, which are assumed to be proportional to transmembrane flow rate F_{vt}, (m^3/s) as

$$C_p' = HF_{vt}^{m} \tag{1}$$

where 'H' is proportionality constant, which depends on particle/solute concentration C_p', and in other words, C_p' is the number of blocked pores. While deriving the laws that govern the fouling mechanism, 'm' will invariably take only positive values in order to imply that the number of particles that block the pores increases with an increase in transmembrane flow rate (F_{vt}, m^3/s).

Different fouling mechanisms can be seen from the schematic diagram shown in Fig. 1. They are complete pore blocking, standard pore blocking, intermediate pore blocking, and cake formation.

Case I: Complete pore-blocking:

In this case, it is assumed that each particle/solute approaching the membrane surface contributes to the blocking of pores. This happens in the event when the size of the particles/solute is larger than the membrane pore size (Fig. 1a). Further, it is assumed that there is no superimposition of particles/solutes one over the other. As a result, the permeate flow rate decreases exponentially with time.

If the number of particles clogging is independent of transmembrane flow rate, F_{vt}, m^3/s, (m = 0 in Eq. (1)) and F_{vt} is assumed to be constant through a given pore until it is partially or completely blocked.

If 'n' pores are remaining unblocked (still open)

$$F_{vt} = n.\ s \tag{2}$$

where, 's' is the flow through one capillary ($s = F_{v0}/n_0$, m^3/s).

The number of pores blocked 'dn' in time 'dt' (as each particle is assumed to clog/block one pore) is given by

$$-\,dn = C_p'dV \tag{2a}$$

but $dF_{vt} = dn.\ s$. Therefore, $dF_{vt} = -C_p'.\ s.\ dV$ so by putting $C_p'.\ s = K_C$ and $dV = F_{vt}.\ dt$, we get

$$dF_{vt} = -K_C.\ F_{vt}.\ dt \tag{2b}$$

where, K_C is constant and given as $K_C = C_p'.s$. Further, C_p' and 's' are constant or remain constant during filtration and K_C, the constant in complete pore-blocking phenomena, represents the reduction in effective membrane surface (due to pore blockage) per unit volume of total permeate.

On integration, it results in an equation for the transmembrane flow rate as a function of time (time law) as

$$F_{vt} = F_{v0}\exp(-K_C.\ t) \tag{2c}$$

The number of blocked pores on the membrane surface increases as the filtration progresses (Hwang & Lin, 2002).

The linearized form of the equation for permeate flow as a function of time is given by

$$\ln F_{vt} = \ln\ F_{v0} - K_C t \tag{2d}$$

Further, since

$$F_{vt} = \frac{dV}{dt} \tag{2e}$$

The above equation can be integrated with an initial condition at t = 0; V = 0 (to obtain the integration constant) to result in relation for the permeate volume (V) as a function of time (t) as

$$V_t = \frac{F_{v0}}{K_C}[1 - \exp(K_C.\ t)] \tag{2f}$$

The characteristic of this pore-blocking mechanism is complete blocking with no superimposition of particles/solute and the characteristic differential equation is given by

$$\frac{d^2t}{dV^2} = K_C\left(\frac{dt}{dV}\right)^2 \tag{2g}$$

Case – II: Standard pore blocking

As depicted in Fig. 1b, in this fouling mechanism, there is every likelihood that the particles/ solutes, smaller than the pore size of the membrane, pass through and get deposited/adsorbed on the pore walls (Bowen et al., 1995). Accordingly, it is termed as internal pore-blocking due to direct adsorption which reduces the effective pore size or pore volume. If these membrane pores are of equal cylindrical shape, this fouling mechanism is known as standard pore-blocking phenomena.

At time 't', when 'n' pores are still open, the permeate flow rate equation is still valid

$F_{vt} = n.\ s$ and $C' = HF_{vt}^{m}$. In this case 'm' is assigned an incremental value of half, (m = 1/2)

$$dF_{vt} = -K_S F_{vt}^{1/2} dV \tag{3}$$

but $dV = F_{vt}dt$

Therefore,

$$dF_{vt} = -K_S F_{vt}^{3/2} dt \tag{3a}$$

where, K_S the constant, which represents the decrease in the cross-sectional area of the pores by virtue of adsorption on the pore walls per unit volume of permeate.

After the separation of variables and on integration employing the initial condition: at t = 0; $F_{vt} = F_{v0}$, we obtain the time dependency relation of permeate flow rate as

$$F_{vt} = \frac{F_{v0}}{\left(1 + \frac{Kst}{2}\sqrt{F_{v0}}\right)^2} \tag{3b}$$

Thus, the linearized form of the equation of transmembrane flow rate versus time is

$$\frac{1}{(F_{vt}^{1/2})} = \frac{1}{(F_{v0}^{1/2})} + \frac{K_S t}{2} \tag{3c}$$

Accordingly, the predicted time function of the permeate volume will be given by

$$V_t = \frac{F_{v0}t}{(1 + K_S\sqrt{F_{v0}t})} \tag{3d}$$

and the characteristic differential equation of this pore-blocking mechanism will be

$$\frac{d^2t}{dV^2} = K_S\left(\frac{dt}{dV}\right)^{\frac{3}{2}} \tag{3e}$$

Case III: Intermediate pore blocking

In this pore-blocking mechanism, it is presumed that some particles/solutes will directly be adsorbed on the pore walls while some can get deposited on the particles/solutes that were already settled on the membrane surface blocking the pores. In this case 'm' is assigned the next incremental value as, m = 1

Accordingly

$$dF_{vt} = -K_I F_{vt}^{2}.\ dt \tag{4a}$$

On integration, after separating the variables and employing the initial condition: at $t = 0$, $F_{vt} = F_{v0}$ to obtain the integration constant.

On integration, we obtained the linearized form of the equation for permeate flow rate versus time as

$$\left(\frac{1}{F_{vt}}\right) = \left(\frac{1}{F_{v0}}\right) + K_I t \tag{4b}$$

Further, the permeate flow rate equation as

$$F_{vt} = \frac{F_{v0}}{(1 + F_{v0}K_I t)} \tag{4c}$$

and the equation for permeate volume as a function of time as

$$V_t = \frac{1}{K}\ln(K_I F_{v0} t + 1) \tag{4d}$$

The characteristic differential equation will take the form as

$$\left(\frac{d^2t}{dV^2}\right) = K_I\left(\frac{dt}{dV}\right) \tag{4e}$$

Case IV: Cake formation

Another possible fouling mechanism could be layer/cake formation as a result of the deposition of particles/solutes on the particles/solutes that have already settled on the membrane surface due to their rejection by the membrane (pores). This situation arises when the particle/solute size is larger than the pore size. In this scenario, as the filtration progresses, the membrane surface uncovered by the particles/solute layer/cake reduces, eventually leaving no free membrane surface (Palacio et al., 2002).

Here the number of particles/solutes blocking the pores (due to their high concentration) are assumed to have a strong dependence on the transmembrane flow rate and accordingly 'm' is assigned a higher value of $m = 2$

Accordingly,

$$dF_{vt} = -K_{CF}F_{vt}^3.\ dt \tag{5}$$

On integration after separating the variables and employing the initial condition as $t = 0$, $F_{vt} = F_{v0}$ to obtain the integration constant, we get the equation for transmembrane flow rate as a function of time as,

$$F_{vt} = \frac{F_{vo}}{\sqrt{1 + 2F_{v0}^2K_{CF}t}} \tag{5a}$$

The linearized form of the equation for flux versus time is

$$\left(\frac{1}{F_{vt}^2}\right) = \left(\frac{1}{F_{v0}^2}\right) + 2K_{CF}t \tag{5b}$$

and the equation for permeate volume versus time as

$$V_t = \left[\frac{1}{K_{CF}F_{v0}}\sqrt{1} + K_{CF}F_{v0}^2.\ t - 1\right] \tag{5c}$$

The characteristic differential equation corresponding to this case is given as

$$\left(\frac{d^2t}{dV^2}\right) = K_{CF}\left(\frac{dt}{dV}\right)^0 = K_{CF} \tag{5d}$$

In the present study, ultrafiltration (UF) and acoustic field-assisted ultrafiltration of TCW were carried out and its effect on transmembrane flux, microbial quality, enzymatic activity and sensory quality of TCW were evaluated. The membrane fouling mechanisms were also evaluated in UF and acoustic field-assisted UF.

3. Materials and methods

3.1. Materials

The tender coconuts (10–15 numbers) of 6–8 months maturity were procured from the local market and water was drawn from them for the conduct of experiments. The plate count agar, potato dextrose agar, and HiCrome *E. coli* agar were purchased from HiMedia Mumbai. All chemicals used for the experiments were of analytical grade. Polyethersulfone membrane (PES 30 and 100 kDa) and stirred cell (UF stirred cell 47 mm XFUF04701, 50 mL capacity) were procured from EMD Millipore Corporation, USA.

3.2. Experimental procedure

Tender coconuts were cleaned thoroughly with tap water to remove dust particles adhered to the surface of the coconuts during transportation and handling. The fruit mesocarp was punctured with the help of a special type of stainless steel knife. The TCW was strained using a muslin cloth to separate coarse particles, if any. The TCW was then pre-filtered through Whatman no. 1 filter paper to remove any suspended particles. The pre-filtered TCW was subjected to ultrafiltration and acoustic field-assisted ultrafiltration. The experimental setup for ultrafiltration and acoustic field-assisted ultrafiltration is shown in Fig. 2.

3.2.1. Ultrafiltration

The ultrafiltration of TCW was carried out with the stirred cell placed inside the laminar flow chamber to avoid contamination during processing. The stirred cell was wiped with 70% ethanol and was exposed to ultraviolet radiation for sterilization before starting the experiments. Ultrafiltration experiments were carried out by employing polyethersulfone (PES) membranes of molecular weight cut-off (MWCO) 30 and 100 kDa at different pressures (1, 2, 3 and 4.5 bar) at constant stirring speed (approx. 100 rpm) and at a temperature of 25 ± 2 °C. The membrane MWCO size was selected based on the molecular weight of enzymes (PPO and POD) present in the TCW. Nitrogen gas was used for the application of transmembrane pressure. Ultrafiltration of TCW was carried out up to 50% reduction in volume, in other words, the volume reduction factor of 2 (VRF = total volume/retentate volume) till the steady-state of flux tends to reach. The retentate and permeate samples were collected for analysis. The volume of permeate was noted at intervals of 30 s and permeate flux was calculated. The water flux was calculated before and after ultrafiltration processing of TCW.

3.2.2. Acoustic field-assisted ultrafiltration

Ultrafiltration of TCW was carried out in the presence of an acoustic field (1.2 MHz) using an ultrasonic transducer (model HM-460, Milford, MA) at 25 ± 2 °C. The stirred cell was placed above the ultrasonic transducer during the experiments and the permeate flow rate of TCW was recorded. Experiments were continued till VRF 2 achieved, and permeate as well as retentate samples were collected for the analysis. The water flux was calculated before and after the acoustic field-assisted ultrafiltration of TCW.

3.3. Permeate flux

Permeate flux is defined as the mass is permitted through the membrane per unit of area and per unit time. Permeate flux was calculated by the following equation.

$$J = \frac{Mp}{A \times t}$$

where, J is the permeate flux (L/m^2/h), M_p (kg) is the mass of permeate at time t (h) and A is the permeation area (m^2).

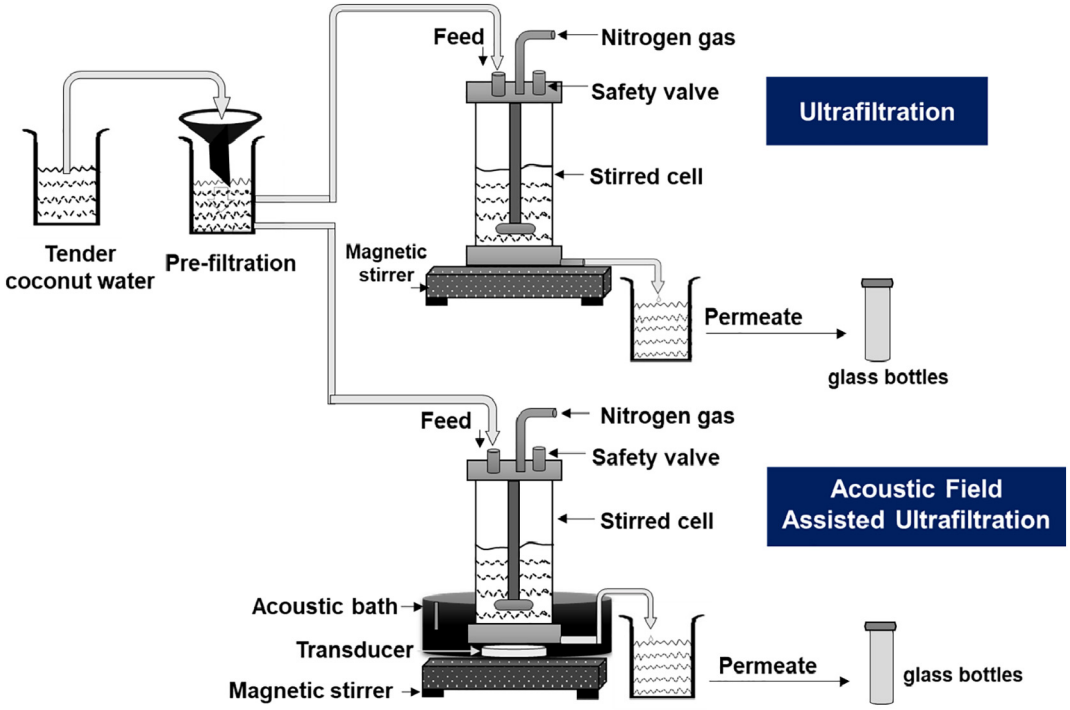

Fig. 2. Experimental setup for ultrafiltration and acoustic field-assisted ultrafiltration of Tender Coconut Water.

3.4. Modelling

Hermia's model was employed to gain insight into the fouling mechanisms occurring during the ultrafiltration of TCW (Hermia, 1982). The different fouling mechanisms complete pore-blocking, standard pore-blocking intermediate pore blocking, and cake formation were evaluated.

3.5. Enzyme activity

3.5.1. Polyphenol oxidase and peroxidase activity

Polyphenol oxidase (PPO) enzyme activity of TCW samples was estimated according to the method described by Campos and Matsui (Campos et al., 1996; Matsui et al., 2008), with some modifications. Sodium phosphate buffer (5.5 mL of 0.2 mol/L, pH 6.0), pyrocatechol (1.5 mL of 0.2 mol/L) and coconut water (1.0 mL) solution was mixed thoroughly, and the change in absorbance was recorded after every 1 min up to 30 min at 425 nm in UV–VIS Spectrophotometer.

Peroxidase (POD) enzyme activity was determined by the method described by Fehrmann & Dimond (1967) with slight modifications. Potassium dihydrogen phosphate buffer solution (7.0 mL of 0.2 mol/L, pH 5.5), guaiacol (1.5 mL of 0.5 g/L), hydrogen peroxide (0.5 mL of 1 mL/L) and coconut water (1.0 mL) solution was mixed thoroughly and change in absorbance was recorded after every 1 min up to 30 min at 470 nm (S.D.B. Spectrophotometer, Model UV-200S Japan).

The absorbance data acquired was plotted against time, and the PPO and POD activities were calculated from the slope.

The percentage of enzyme activity in retentate was calculated by the following formula.

$$R(\%) = 100 \times \left(1 - \frac{EA_p}{EA_f}\right)$$

where, R is percentage retention, EA_p is enzyme activity in permeate and EA_f is the enzyme activity in the feed (Debien, Gomes, Ongaratto, & Viotto, 2013).

3.6. Microbiological analysis

Plate count agar, potato dextrose agar and HiChrome *E. coli* agar were used to determine the total aerobic mesophilic plate count, yeast and mold counts, and *E. coli* count of coconut water, respectively. Nearly 15–20 mL medium was poured into sterile Petri plates and allowed to solidify. TCW samples were plated on to the medium in Petri plates by spread plate method. The plates were incubated for 20–24 h for total plate count and 48 h for *E. coli* at 37 ± 2 °C. Plates with potato dextrose agar media were incubated for 3–4 days at room temperature 27 ± 2 °C (Thapa, Pal, & Tamang, 2004). All the experiments were carried out in triplicates, and average values are reported.

3.7. Physicochemical analysis

Physicochemical parameters (namely pH, total titratable acidity, TSS, density, and particle size) of TCW before and after membrane processing were analysed. The pH of retentate and permeate samples were measured using digital pH meter (Eutech Instruments pH 510, Singapore). The total titratable acidity of samples was analysed by titration against 0.1 N NaOH solution and phenolphthalein as an indicator (Ranganna, 1986). Total soluble solids (TSS) were measured by a digital refractometer. The density of all samples was calculated as weight/unit volume. The protein content of TCW was analysed by using an N-protein analyser (Thermo Flash 2000, Waltham, Massachusetts). The fat and ash content of TCW was evaluated according to the AOAC procedure (AOA, 2000). The total sugar content of the samples was determined by the phenol-sulphuric acid method (Nielsen, 2010). All the analyses were carried out in triplicate, and the mean values are presented.

3.8. Turbidity

The turbidity of samples was analysed by employing UV–VIS Spectrophotometer (S.D.B. Spectrophotometer, Model UV-200S Japan) at 610 nm. Absorbance (A_b) of the samples was recorded in reference to distilled water. The transmittance (T_r) and turbidity (*Tur*) were

calculated by the following equations (Matsui et al., 2008).

Transmittance $(Tr) = 100 \times (10^{-Ab})$

Turbidity $(Tur) = 100 - Tr$

3.9. Sensory analysis

Sensory attributes of fresh and membrane processed TCW were evaluated on a nine-point hedonic scale and was compared with thermally processed TCW (market sample). All the samples were coded, and sensory evaluation was carried out on the basis of parameters such as appearance, colour, aroma/flavour, taste, turbidity, aftertaste, mouthfeel and overall acceptability. Sensory analysis of samples was performed by trained panellists using nine-point Hedonic rating scale, representing their degrees of like to dislike. Average scores for each parameter are described in the results.

4. Results and discussion

The ultrafiltration of tender coconut water (TCW) was carried out at four different pressures (1, 2, 3 and 4.5 bar) using a 50 mL working volume in a cell at fixed stirring speed (≈100 rpm) and ambient temperature (25 ± 2 °C). The flow rate (volume versus time) of permeate was noted until volume reduction factor (VRF) of 2 is reached. Acoustic field-assisted ultrafiltration of TCW was also carried out at similar operating conditions.

Physicochemical properties of permeate samples were evaluated, besides its enzyme activity and microbial analysis. The effect of various parameters such as transmembrane pressure, molecular weight cut-off (MWCO) and acoustic-field on permeate flux was evaluated and the results are presented and discussed in the following subsections.

4.1. Ultrafiltration

4.1.1. Effect of transmembrane pressure

The effect of transmembrane pressure (1, 2, 3 and 4.5 bar) on the permeate/transmembrane flux (m/s) in the case of 30 and 100 kDa membrane during ultrafiltration of TCW can be seen from Fig. 3.

The permeate flux was recorded during ultrafiltration and significant effect was observed with an increase in transmembrane pressure over a period of time. However, the extent of increase in the flux decreased with an increase in transmembrane pressure. For instance, an increase of 21.82% in permeate flux was observed with an increase of transmembrane pressure from 1 to 2 bar, whereas only 7.56 and 5.18% increase was observed with an increase in pressure from 2 to 3 bar and 3 to 4.5 bar, respectively.

As anticipated, a steep decline in transmembrane flowrate was observed at the beginning of ultrafiltration at all four transmembrane pressures which can be attributed to pore blocking (fouling). However, the slower rate of decrease in flux with further processing time (tending to steady-state) might be due to the accumulation of solutes on membrane surface resulting in concentration polarisation and eventually cake formation (Grenier, Meireles, Aimar, & Carvin, 2008; Sarkar, 2013).

4.1.2. Effect of molecular weight cut-off

The effect of molecular weight cut-off (MWCO), on permeate flux, two different MWCO (30 and 100 kDa) membranes were used for the ultrafiltration of TCW was evaluated, and results are shown in Fig. 3.

Mostly, higher MWCO membranes required less time for ultrafiltration compared to the lower MWCO membranes due to an increase in permeate flux. The same can be seen from the figure that UF employing 100 kDa membrane exhibited higher permeate flux when compared to that of UF using 30 kDa membrane at all applied pressures. The time required to achieve the volume reduction factor (VRF) 2, significantly decreased with an increase in membrane MWCO and applied pressures.

4.1.3. Effect of ultrasonication

The effect of the application of the acoustic field on permeate flux during ultrafiltration (with 30 kDa membrane) was evaluated and the results are presented in Fig. 4. The acoustic field used in the present study is in the MHz range and completely different from the kHz range acoustic field (Narayan et al., 2002). It can be seen from the figure that the time required to reach VRF of 2 was observed to lessen in the presence of ultrasonication. This can be appreciated by the fact that at any given time during the ultrafiltration process, the permeate flux was higher in the presence of ultrasonication (over ultrafiltration alone).

The permeate flux during acoustic field-assisted ultrafiltration was noted, and with an increase in transmembrane pressure, a significant increase in permeate flux was observed, over a period of time. However, the extent of increase in the permeate flux decreased with an increase in transmembrane pressure. For instance, 14.49% rise was observed in permeate flux when pressure was increased from 1 to 2 bar, whereas only 12.79 and 9.09% increase was observed with an increase in transmembrane pressure from 2 to 3 bar and 3 to 4.5 bar. Similar results were also observed when 100 kDa MWCO membrane was employed under otherwise similar conditions.

The increase in permeate flux in the presence of ultrasonication can be attributed to the fact that ultrasonic streaming of magnitude in the

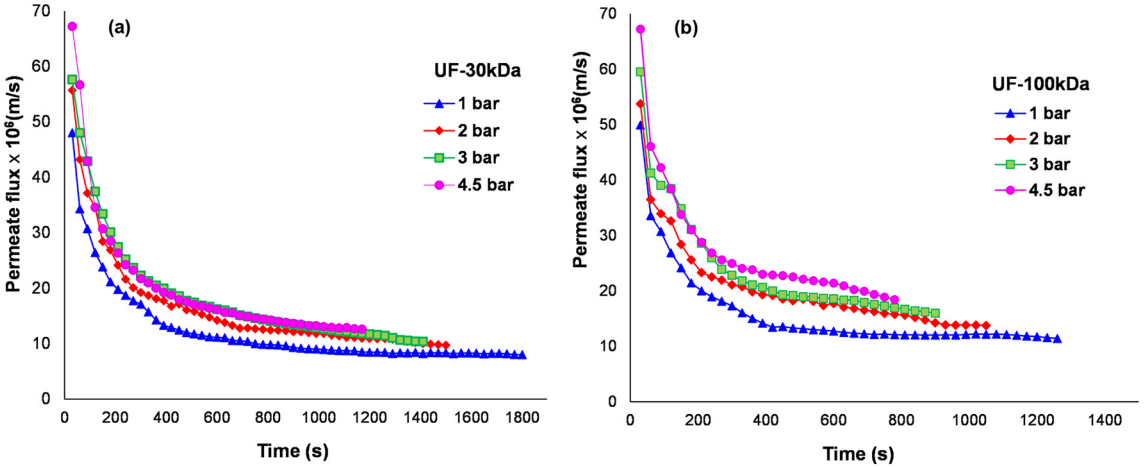

Fig. 3. Effect of different transmembrane pressures on permeate flux during ultrafiltration (UF) of Tender Coconut Water with (a) 30 kDa, (b) 100 kDa MWCO PES membrane.

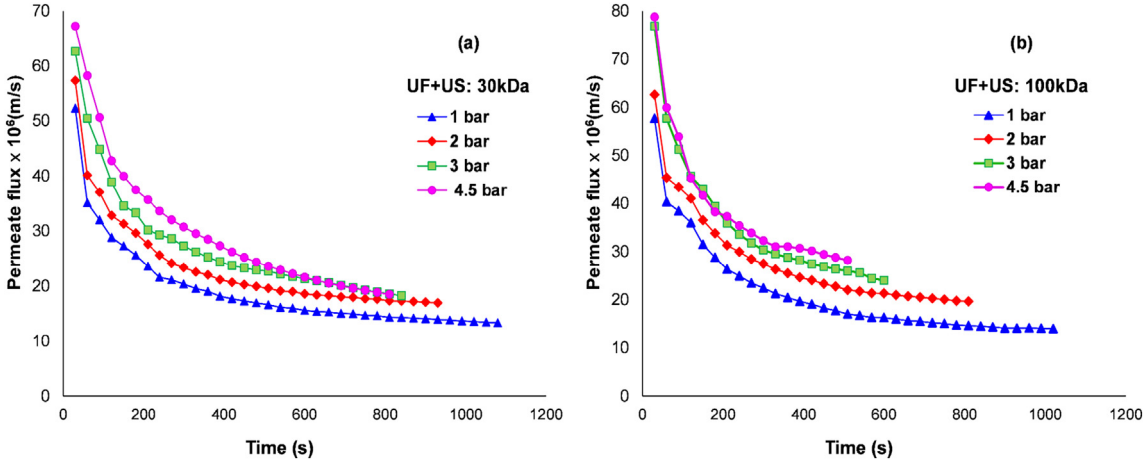

Fig. 4. Effect of application of acoustic field (UF + US) on permeate flux Vs time at different transmembrane pressures during ultrafiltration (UF) of Tender Coconut Water with (a) 30 kDa & (b) 100 kDa MWCO PES membrane.

range of micrometres or even smaller agitate the aqueous medium and creates microbubbles. This agitation provides an additional force (turbulence) capable of disrupting/disturb the concentration polarisation layer and removes the particles from the membrane surface (Jin et al., 2014; Juang & Lin, 2004; Narayan et al., 2002). Ultrasound creates an alternating adiabatic compression and rarefaction cycle, resulting in cavitation near to the membrane surface (in liquid medium). Cavitation comprises of rarefaction cycle and compression cycle of the ultrasonic wave. Rarefaction creates negative pressure leading to formation and growth of the microbubbles, whereas, compression cycle results in the collapse of bubbles (Mittal, Tavanandi, Mantri, & Raghavarao, 2017; Simon et al., 2000). The collapse of the bubbles releases energy in the liquid medium and creates convective currents causes agitation/convection between the boundary layer and bulk solution. This agitation has an impact on the interactions between foulant and membrane surface, causing the fracture and removing the fouling film from the surface and/or from inside of pores of the polymer membrane causing cleaning of the membrane.

Ábel et al. (2015) have studied ultrasound-assisted ultrafiltration of milk whey solution and found an increase in permeate flux with a decrease in the concentration polarisation layer. The increase in transmembrane flux has been reported with the application of the acoustic field during osmotic membrane distillation of sugarcane juice (Narayan et al., 2002). The problem of membrane fouling was reported to be addressed by the application of ultrasonication. This is due to the high-velocity fluid movement associated with ultrasonication and acoustic streaming (Lamminen, Walker, & Weavers, 2004).

The water flux was evaluated before and after the membrane processing of tender coconut water. A significant decrease was observed in the performance of the membrane after membrane processing and the results are shown in Fig. 5.

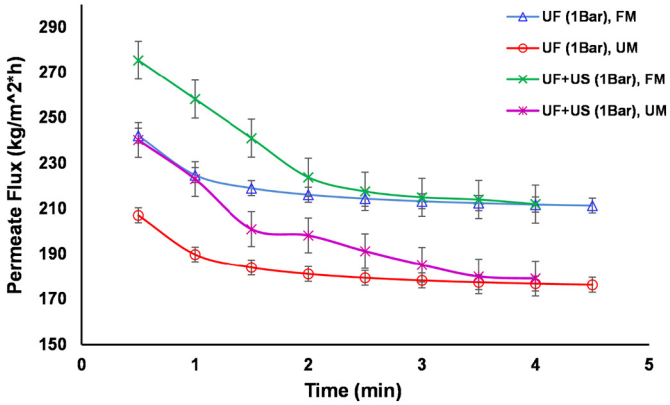

Fig. 5. Water flux before and after ultrafiltration and ultrasonication of Tender Coconut Water (UF: Ultrafiltration, UF + US: Ultrafiltration + Ultrasonication, FM: Fresh membrane, UM: Used Membrane, TMP: 1 bar, MWCO: 30 kDa PES membrane).

4.2. Membrane fouling mechanism

During the ultrafiltration of TCW, some membrane fouling occurs, resulting in a decline in permeate flux. This can be attributed to the presence of polysaccharides, enzymes and proteins present in TCW. In the present study, Hermia's model was employed to gain insight into the fouling mechanisms occurring during the ultrafiltration of TCW. The equations representing the mechanisms of complete pore blocking, standard pore-blocking, intermediate pore-blocking, and cake formation are given in Table 1 along with the blockage patterns, parameters and exponent values (n) for each model. Schematic representation of different membrane fouling mechanisms or blocking patterns during ultrafiltration is shown in Fig. 1. The flux values corresponding to equations of different fouling mechanisms during ultrafiltration and acoustic field ultrafiltration are presented in Figs. 3 to 6. The corresponding R^2 values and fitted parameters are given in Tables 2 and 3.

For any model, a high R^2 value represents a good fit of experimental data. In the present study, the degree of fit (R^2 value) was observed to increase and then decrease with an increase in transmembrane pressure for any fouling mechanism. This could be due to passage of perhaps more solutes into the pores leading to more of intermediate pore blocking while some of them even come out into the permeate with further increase in pressure. The extent of an increase in transmembrane flux is increasing and decreasing with an increase in transmembrane pressure. This observation can be supported by the increase of turbidity values in permeate with an increase in transmembrane pressure (discussed in Section 4.6). Based on the R^2 value, the best fit was observed in the case of cake formation. It can be observed from Table 2; the values of R^2 are rather low for any given mechanism that was considered in describing the fouling mechanism. One reason for this deviation in complete matching in predicting the effect of parameters on the performance could be the real structure of membrane pores. The real situation pre structure of the membrane perhaps could be a zigzag (irregular/asymmetric) structure (Fig. 7) rather than a cylinder as assumed earlier (Fu & Zhang, 2019; Habib et al., 2013). However, cake formation has an extremely low coefficient (3–4 $\times$ 10^{-5} s/m) indicating it to be the least significant mechanism of fouling. This paradox can be resolved in the following manner.

Table 1
Brief information on Hermia's Membrane fouling/ blocking mechanism models.

Type of fouling	Complete pore blocking	Standard pore blocking	Intermediate pore blocking	Cake formation
Modelling equation	$\ln F_{vt} = \ln F_{v0} - K_C t$	$\frac{1}{(F_{vt}^{1/2})} = \frac{1}{(F_{v0}^{1/2})} + \frac{K_S t}{2}$	$\left(\frac{1}{F_{vt}}\right) = \left(\frac{1}{F_{v0}}\right) + K_I t$	$\left(\frac{1}{F_{vt}^2}\right) = \left(\frac{1}{F_{v0}^2}\right) + 2K_{CF} t$
Parameters for model fit	K_C	K_S	K_I	K_{CF}
Exponent n	2	1.5	1	0
No. of equation	2d	3c	4b	5b
Blockage pattern	Sealing of pores	Restriction of pore walls	Sealing of pores and deposition on the membrane surface	Cake layer formation on the membrane surface

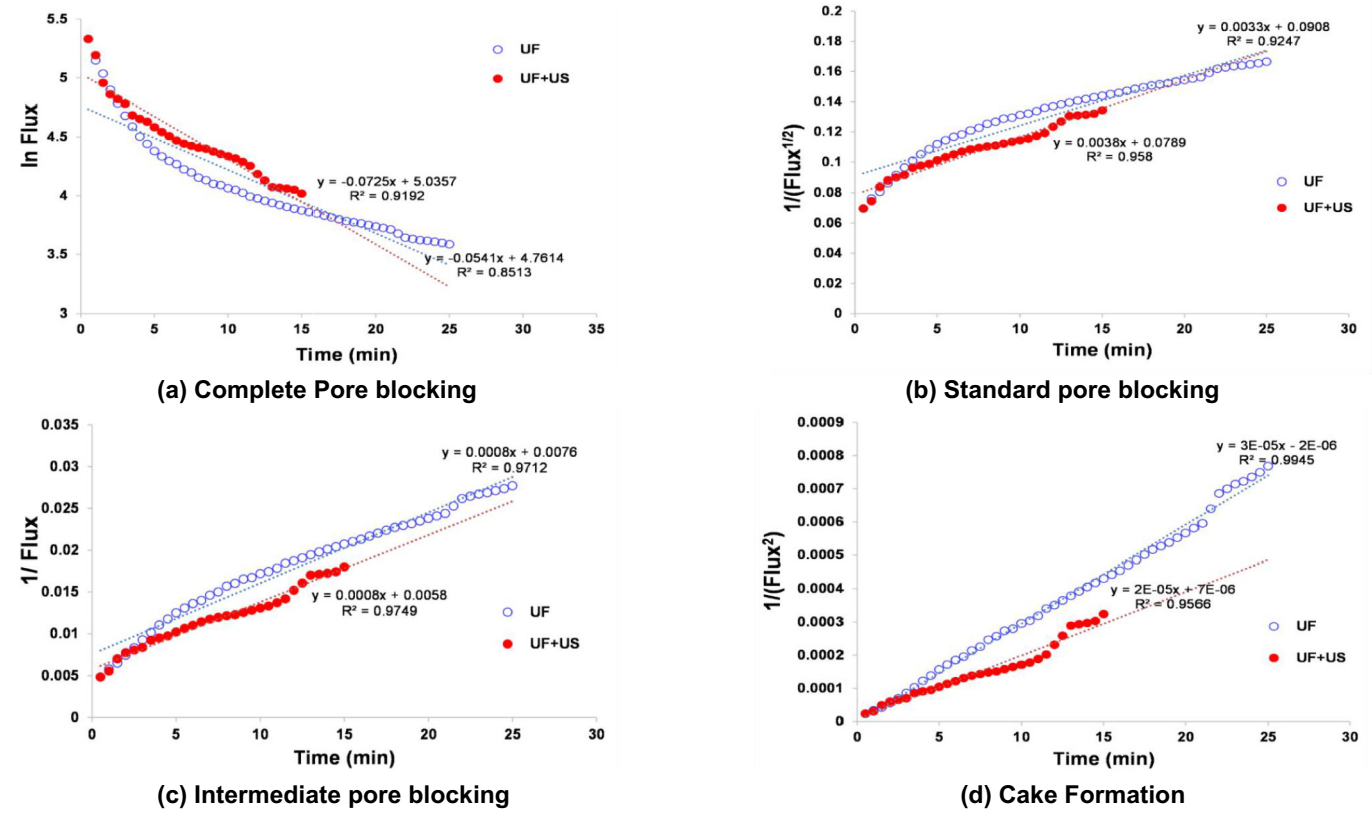

Fig. 6. Fouling mechanisms during ultrafiltration of Tender Coconut Water at 3 bar TMP (a) Complete pore-blocking (b) Standard pore-blocking (c) Intermediate pore-blocking (d) Cake Formation (Membrane: PES, MWCO: 30 kDa).

Table 2
The R^2 value obtained from the experimental data to study the effect of ultrafiltration and the combination of ultrafiltration with ultrasonication on membrane fouling.

	Conditions	1 bar		2 bar		3 bar		4.5 bar	
		30 kDa	100 kDa	30 kDa	100 kDa	30 kDa	100 kDa	30 kDa	100 kDa
Complete pore-blocking (n = 2)	UF	0.6957	0.6376	0.7628	0.7412	0.8513	0.7916	0.7810	0.7807
	UF + US	0.7903	0.8242	0.8859	0.8625	0.9192	0.8585	0.9270	0.7142
Standard pore-blocking (n = 1.5)	UF	0.7604	0.6812	0.8215	0.8135	0.9247	0.8518	0.8657	0.8447
	UF + US	0.8553	0.8839	0.9386	0.9105	0.9580	0.9060	0.9662	0.7782
Intermediate pore-blocking (n = 1)	UF	0.8427	0.7470	0.9015	0.9025	0.9712	0.8999	0.9257	0.8958
	UF + US	0.9055	0.9284	0.9705	0.9690	0.9749	0.9423	0.9895	0.8337
Cake formation (n = 0)	UF	0.9194	0.8186	0.9873	0.9718	0.9945	0.9618	0.9873	0.9590
	UF + US	0.9677	0.9791	0.9821	0.9749	0.9925	0.9842	0.9965	0.9160

UF: Ultrafiltration, UF + US: Ultrafiltration with acoustic field-assisted Ultrasonication.

It can be inferred that complete pore-blocking is the actual mechanism, and in association with concentration polarisation, is responsible for the flux decline in the ultrafiltration of TCW. Complete pore blocking or concentration polarisation has a similar effect on flux like cake formation. The only difference between complete pore blocking and cake formation is that no layer formation is present in complete pore blocking. The difference between concentration polarisation and cake formation is that the former is the boundary layer in

Table 3
The fitted Hermia's model parameters to study the effect of ultrafiltration and the combination of ultrafiltration with ultrasonication on membrane fouling.

MWCO (kDa)	Pressure (bar)	Parameters for model fit							
		Complete pore blocking		Standard pore blocking		Intermediate pore blocking		Cake formation	
		K_C (s^{-1})		K_S ($s^{-1/2}$ $m^{-1/2}$)		K_I (m^{-1})		K_{CF} (s m^{-2})	
		UF	UF + US	UF	UF + US	UF	UF + US	UF	UF + US
30	1	0.0402	0.0474	0.0026	0.0028	0.0009	0.0007	4E−05	2E−05
	2	0.0621	0.0467	0.0028	0.0034	0.0008	0.0008	3E−05	2E−05
	3	0.0541	0.0725	0.0033	0.0038	0.0008	0.0008	3E−05	2E−05
	4.5	0.0661	0.0866	0.0037	0.0041	0.0009	0.0008	3E−05	2E−05
100	1	0.0439	0.0647	0.0026	0.0036	0.0007	0.0008	2E−05	2E−05
	2	0.0540	0.0721	0.0033	0.0046	0.0007	0.0008	2E−05	2E−05
	3	0.0654	0.0996	0.0035	0.0043	0.0007	0.0008	2E−05	1E−05
	4.5	0.0719	0.0866	0.0035	0.0036	0.0007	0.0006	1E−05	9E−06

UF: Ultrafiltration, UF + US: Ultrafiltration with acoustic field-assisted Ultrasonication, MWCO: Molecular weight cut-off.

which the solute concentration gradient develops, while cake formation is a layer of solids accumulates one over the other over a period of time. Another factor that lends support to this line of argument is that cake formation is prominent at higher processing time, whereas concentration polarisation is effective right from the beginning of ultrafiltration.

Yet another aspect that supports this hypothesis is the flux enhancement in the presence of ultrasonication. It is known that ultrasonication (MHz) disturbs the concentration polarisation layer and enhances the flux (Narayan et al., 2002). It is unlikely that ultrasonication has any bearing on the solid layers (which occurs in cake formation).

Thus, it can be ultimately concluded that the significant mode of resistance causing flux decline is due to complete pore-blocking and concentration polarisation. The highest values of model parameters observed in complete pore blocking followed by standard pore blocking, intermediate pore blocking and cake formation (Table 3).

The similar trend was observed even in ultrafiltration and acoustic field-assisted ultrafiltration of TCW employing 100 kDa membrane for all the fouling mechanisms. However, a lower degree of fit indicates the fact that some of the small molecular weight solutes pass through 100 kDa membrane.

4.3. Enzyme activity

The enzyme activity (polyphenol oxidase and peroxidase) in fresh, permeate and retentate samples, obtained during ultrafiltration of TCW was analysed and results are presented in Fig. 8. The polyphenol oxidase (PPO) and peroxidase (POD) activity of TCW after ultrafiltration (permeate) were observed to decrease by 95.10% (from 2.45 to 0.12 U/mL) and 97.89% (from 2.38 to 0.050 U/mL), respectively. The ultrafiltration was found to be effective in retaining enzymes in the retentate and resulting in a significant reduction of enzyme activities (PPO and POD) of TCW (permeate).

The application of the acoustic field during ultrafiltration resulted in an insignificant difference in PPO and POD activity (permeate samples) when compared to ultrafiltration alone. However, in retentate, the reduction in PPO and POD enzyme activity was observed in the retentate (nearly 30%). This could be attributed to the fact that retentate was

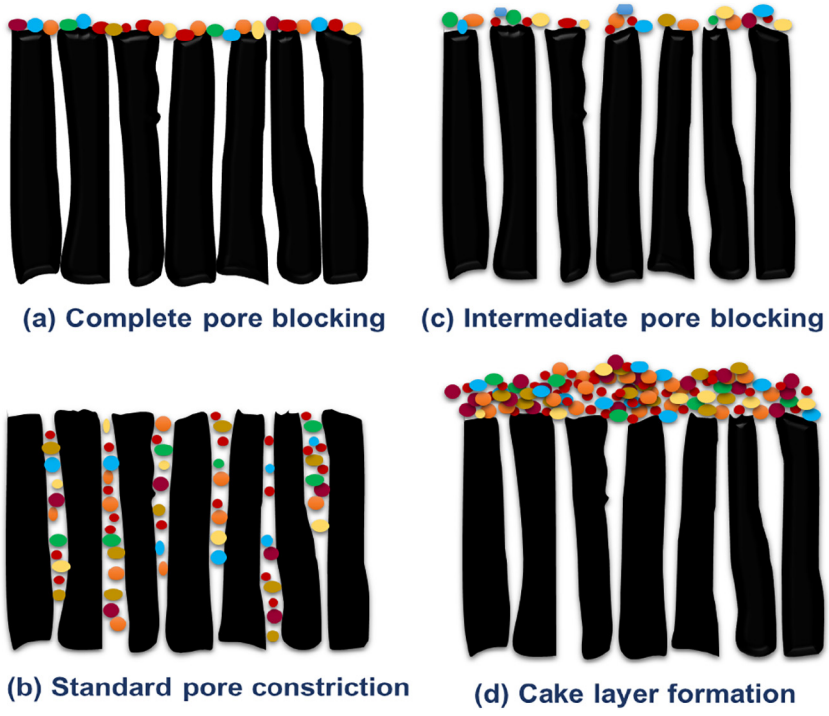

Fig. 7. Schematic representation of real structure (zigzag/asymmetric) structure of membrane.

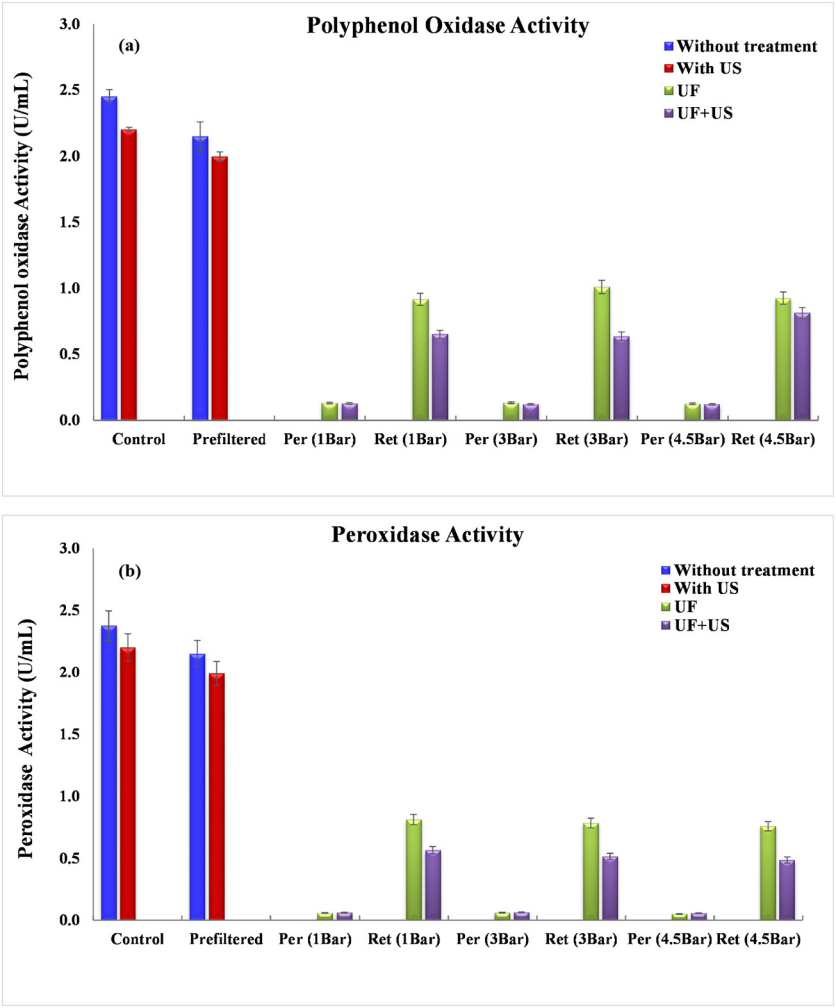

Fig. 8. Effect of membrane processing on (a) polyphenol oxidase and (b) peroxidase enzyme activity of tender coconut water.

exposed to ultrasonication for a longer period.

Similar results for enzyme activity results are reported in literature by Debien et al. for fresh and ultrafiltered (by polyethersulphone 150 kDa membrane) TCW were 2.61 and 0.39 U/mL (PPO) and 7.22 and 1.56 U/mL (POD), respectively (Debien et al., 2013). The PPO and POD enzyme activity of fresh TCW were 5 and 0.3 U/mL (Duarte, Coelho, & Leite, 2002). The enzyme activity values of fresh TCW reported were much higher (32.1 and 114.3 U/mL for PPO and POD), which can be attributed to geographical factors (Campos et al., 1996).

4.4. Microbial load

The values of the microbial load of TCW samples before and after ultrafiltration are presented in Fig. 9. *E. coli* test was found to be negative for all the samples. The bacterial count of the control sample (fresh TCW exposed to the environment during collection) was found to be 4.16 log CFU/mL (Fig. 9a). The total plate count of fresh TCW reported was 2.27 log CFU/mL (Kailaku, Setiawan, & Sulaeman, 2017).

It can be seen from the figure that the total plate count of TCW (permeate) samples decreased significantly (from 4.05 to 0.00 log CFU/mL) after ultrafiltration (with 30 kDa membrane) achieving cold sterilization. Ultrafiltered TCW stored for three months at refrigerator conditions also showed zero microbial count. The retentate obtained during ultrafiltration and acoustic field-assisted ultrafiltration were found to have total plate count in the range of 3.0–3.54 log CFU/mL. The lower total bacterial count in the latter can be attributed to microbial inactivation by ultrasonication. These results are comparable to those reported in the literature. It was reported that the total plate count for fresh TCW was 2.15 log CFU/mL and no microbial load in micro-filtered TCW (Mahnot, Kalita, Mahanta, & Chaudhuri, 2014). However, it was observed that the microfiltration was not able to achieve complete removal of microbes in TCW (employing 0.45 μm membrane) (Purkayastha et al., 2012).

Another microbial parameter that is 'yeast and mold' count for all the samples was analysed and the results are presented in Fig. 9b. The 'yeast and mold' count of the control sample (fresh TCW) was found to be 4.14 log CFU/mL. Complete reduction in the microbial count (100%) was observed in permeate samples after ultrafiltration as well as acoustic field-assisted ultrafiltration, at all applied pressures. The retentate samples indicated yeast and mold count in the range 2.58–3.15 log CFU/mL. The total bacterial count and yeast and mold count of fresh coconut water (exposed to environment) reported were 6.54 and 5.63 log CFU/mL, respectively (Reddy, Das, & Das, 2007).

4.5. Physicochemical properties

Fresh and ultrafiltered TCW samples were analysed for physicochemical properties (density, total soluble solids, pH and titratable acidity) and results are presented in Table 5. A significant difference was not observed in density, pH and titratable acidity of TCW after ultrafiltration except a slight difference in total soluble solid content. These results are similar to the literature reports in terms of pH (4.5–6.5), TSS (4.0–5.29) and titratable acidity (0.04–0.149%) for fresh TCW (Chowdhury et al., 2005; Debien et al., 2013; Mahnot et al., 2014;

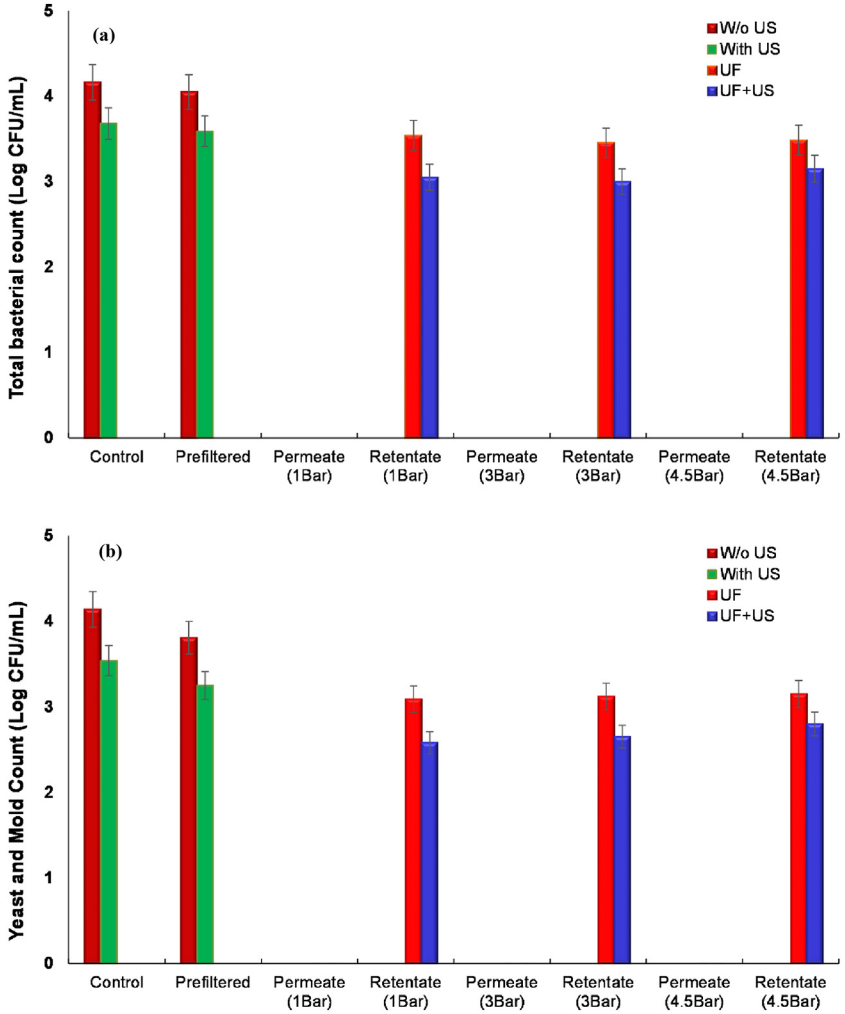

Fig. 9. Effect of membrane processing on (a) Total bacterial count and (b) Yeast and mold count of tender coconut water.

Matsui et al., 2008).

The fresh TCW was analysed and estimated to have 0.05% protein, 0.45% fat, 0.56% ash and 4.25% total sugars. On ultrafiltration, employing 30 and 100 kDa membranes, a slight decrease in the protein (0.048 and 0.049%), fat (0.42 and 0.44%) and total sugar content (4.21 and 4.24%) was observed whereas no significant difference was observed in ash content (0.56%) (Table 4).

4.5.1. Turbidity

The turbidity of TCW subjected to ultrafiltration and acoustic field-assisted ultrafiltration was evaluated, and the results are presented in Fig. 10. It can be observed from the figure that the turbidity of permeate samples was observed to reduce significantly (3.30 to 0.14%). The turbidity values were observed to be lowest (0.14%) in permeate samples obtained at 1 bar transmembrane pressure and increased at higher transmembrane pressures. This can be due to the passage of some components (such as enzymes) through the membrane with an increase in applied pressure. The difference in turbidity was also confirmed by visual comparison in terms of transparency and clarity of control, permeate and retentate samples obtained after membrane processing. Application of the acoustic field did not show much difference in the turbidity values. Decrease in turbidity values of tender (green) coconut water after membrane processing was reported (Debien et al., 2013).

Table 4
Nutritional composition of tender coconut water (TCW).

Parameter	Fresh TCW	Permeate TCW (30 kDa)	Permeate TCW (100 kDa)
Protein (%, w/v)	0.05 ± 0.00	0.05 ± 0.00	0.05 ± 0.00
Fat (%, w/v)	0.45 ± 0.00	0.44 ± 0.01	0.45 ± 0.01
Ash (%, w/v)	0.56 ± 0.01	0.55 ± 0.00	0.56 ± 0.00
Total sugar (%, w/v)	4.25 ± 0.03	4.21 ± 0.02	4.24 ± 0.01

All data reported are the mean of triplicate measurements ± standard deviation.

4.6. Sensory evaluation

The sensory evaluation of ultrafiltered TCW was carried out and compared with that of thermally processed samples and the results are presented in Fig. 11. It can be seen from the figure that the sensorial quality of membrane processed samples was observed to be similar to that of fresh TCW. Also, permeate sample of membrane processed TCW exhibited higher acceptability compared to thermally processed samples. Storage study of membrane processed TCW (permeate) for three months at refrigerated conditions was carried out and found to have good sensorial acceptability. Practically no reports are available on sensory evaluation of membrane processed TCW. However, good overall acceptability of TCW subjected to microfiltration was reported (Mahnot et al., 2014; Purkayastha et al., 2012).

Table 5
Physicochemical properties of fresh and processed tender coconut water.

Processing conditions	Pressure (bar)	Sample	pH	TA (%)	Density (g/mL)	TSS (°Brix)
		Control	5.24 ± 0.01	0.14 ± 0.05	1.003 ± 0.01	3.26 ± 0.41
		Pre-filtered	5.24 ± 0.01	0.14 ± 0.05	1.002 ± 0.02	3.20 ± 0.02
UF	1	Permeate	5.23 ± 0.005	0.14 ± 0.00	1.003 ± 0.01	3.10 ± 0.18
		Retentate	5.24 ± 0.005	0.15 ± 0.07	1.005 ± 0.00	3.20 ± 0.12
	2	Permeate	5.23 ± 0.01	0.14 ± 0.02	1.000 ± 0.01	3.10 ± 0.05
		Retentate	5.23 ± 0.05	0.14 ± 0.02	1.00 ± 0.016	3.14 ± 0.02
	3	Permeate	5.24 ± 0.005	0.13 ± 0.02	1.015 ± 0.00	3.12 ± 0.13
		Retentate	5.22 ± 0.005	0.13 ± 0.02	1.00 ± 0.016	3.15 ± 0.09
	4.5	Permeate	5.23 ± 0.005	0.14 ± 0.01	1.011 ± 0.01	3.15 ± 0.11
		Retentate	5.23 ± 0.005	0.13 ± 0.02	1.00 ± 0.005	3.15 ± 0.15
UF + US	1	Permeate	5.22 ± 0.007	0.15 ± 0.03	1.001 ± 0.001	3.13 ± 0.12
		Retentate	5.21 ± 0.008	0.14 ± 0.01	1.007 ± 0.002	3.20 ± 0.08
	2	Permeate	5.20 ± 0.05	0.14 ± 0.01	1.000 ± 0.011	3.19 ± 0.01
		Retentate	5.20 ± 0.00	0.14 ± 0.02	1.012 ± 0.002	3.18 ± 0.07
	3	Permeate	5.19 ± 0.06	0.13 ± 0.00	1.015 ± 0.011	3.15 ± 0.01
		Retentate	5.18 ± 0.00	0.14 ± 0.00	1.013 ± 0.009	3.18 ± 0.09
	4.5	Permeate	5.22 ± 0.06	0.13 ± 0.01	1.010 ± 0.001	3.15 ± 0.16
		Retentate	5.19 ± 0.00	0.13 ± 0.021	1.013 ± 0.009	3.16 ± 0.02

UF: Ultrafiltration, UF + US: Ultrafiltration with acoustic field-assisted Ultrasonication, TA: titratable acidity, TSS: total soluble solids. Values are averages ± standard deviation from three replicate analyses.

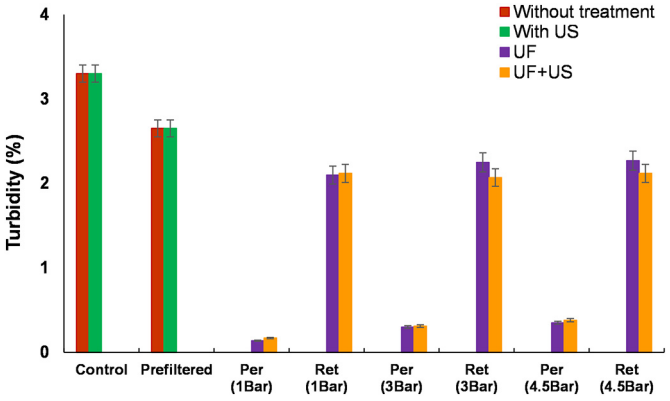

Fig. 10. Effect of membrane processing on turbidity of tender coconut water.

5. Conclusions

The membrane processing (ultrafiltration and acoustic field-assisted ultrafiltration) of tender coconut water (TCW) was carried out at four transmembrane pressures (1, 2, 3, 4.5 bar) and two molecular weight cut-offs (30 and 100 kDa). A clean, green and energy-efficient membrane-based processing method was developed for cold sterilization of TCW (with 30 kDa MWCO membrane) as an alternative to thermal processing. Transmembrane flux increased significantly (30–50%) by the application of ultrasonication. Fouling mechanisms were evaluated and complete pore-blocking was inferred to be the most significant mechanism. In association with concentration polarisation, it is found to be responsible for the decline in permeate flux during ultrafiltration. Ultrafiltration of TCW resulted in a significant decline in enzyme activity (decline in PPO and POD by 95.10% and 97.89%, respectively) and turbidity by 95.81% in permeate samples. The overall acceptability of membrane processed TCW (after three months of storage) was high and close to fresh tender coconut water, indicating the commercial

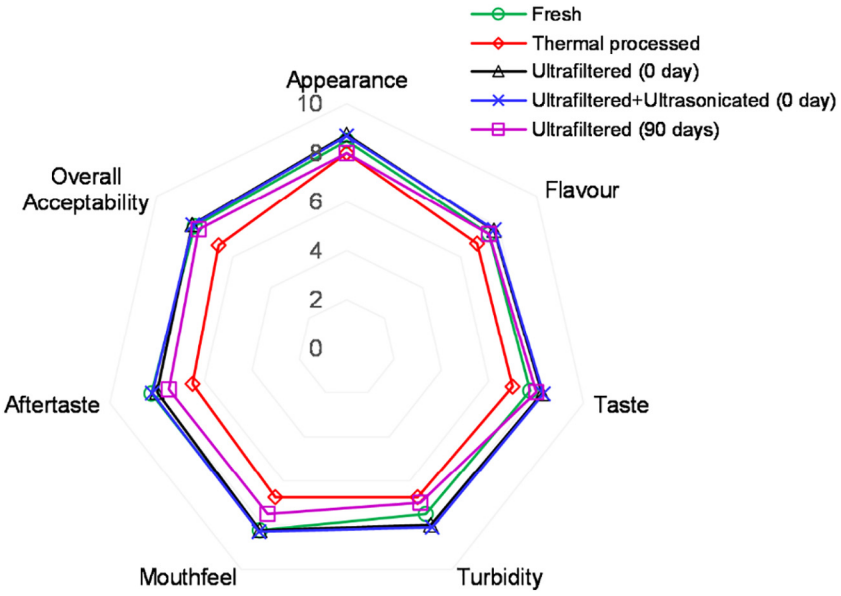

Fig. 11. Effect of membrane processing on Sensory evaluation of tender coconut water.

feasibility of the membrane-based process.

CRediT authorship contribution statement

Archana G. Lamdande: Conceptualization, Data curation, Investigation, Formal analysis, Writing - original draft. **Rochak Mittal:** Methodology, Investigation, Writing - review & editing. **Raghavarao K.S.M.S.:** Supervision, Validation, Writing - review & editing.

Declaration of competing interest

The authors declare no conflict of interest.

Acknowledgements

The authors wish to thank the Director, CSIR-CFTRI, for the infrastructural facilities at the institute. Archana G. Lamdande acknowledges University Grants Commission (UGC), Government of India, for providing the fellowship. Rochak Mittal acknowledges Council of Scientific and Industrial Research (CSIR), Government of India, for providing the fellowship.

References

Ábel, M., Kiss, Z. L., Beszédes, S., Hodúr, C., Keszthelyi-Szabó, G., & László, Z. (2015). Ultrasonically assisted ultrafiltration of whey solution. *Journal of Food Process Engineering, 38*(5), 467–473.

AOA, C. (2000). *Association of official analytical chemists. Official methods of analysis.* 12.

Babu, P. R., & Gaikar, V. (2001). Membrane characteristics as determinant in fouling of UF membranes. *Separation and Purification Technology, 24*(1–2), 23–34.

Baldasso, C., Barros, T., & Tessaro, I. (2011). Concentration and purification of whey proteins by ultrafiltration. *Desalination, 278*(1–3), 381–386.

Bowen, W., Calvo, J., & Hernandez, A. (1995). Steps of membrane blocking in flux decline during protein microfiltration. *Journal of Membrane Science, 101*(1–2), 153–165.

Campos, C. F., Souza, P. E. A., Coelho, J. V., & Gloria, M. B. A. (1996). Chemical composition, enzyme activity and effect of enzyme inactivation on flavor quality of green coconut water. *Journal of Food Processing and Preservation, 20*(6), 487–500.

Cassano, A., Marchio, M., & Drioli, E. (2007). Clarification of blood orange juice by ultrafiltration: Analyses of operating parameters, membrane fouling and juice quality. *Desalination, 212*(1–3), 15–27.

Chowdhury, M., Aziz, M., & Uddin, M. (2005). Development of shelf-stable ready-to-serve green coconut water. *Biotechnol, 4*, 121–125.

Corbatón-Báguena, M.-J., Álvarez-Blanco, S., & Vincent-Vela, M.-C. (2018). Evaluation of fouling resistances during the ultrafiltration of whey model solutions. *Journal of Cleaner Production, 172*, 358–367.

Debien, I. C., Gomes, M. T. S., Ongaratto, R. S., & Viotto, L. A. (2013). Ultrafiltration performance of PVDF, PES, and cellulose membranes for the treatment of coconut water (Cocos nucifera L.). *Food Science and Technology, 33*(4), 676–684.

Duarte, A., Coelho, M., & Leite, S. (2002). Identification of Peroxidase and Tyrosinase in Green Coconut Water Identificación De Peroxidasa Y Tirosinasa En Jugo De Coco Verde Identificación De Peroxidasa E Tirosinasa En Xugo De Coco Verde. *CYTA-Journal of Food, 3*(5), 266–270.

Fehrmann, H., & Dimond, A. (1967). Peroxidase activity and Phytophthora resistance in different organs of potato plant. *Phytopathology, 57*(1), 69.

Fu, W., & Zhang, W. (2019). Chemical aging and impacts on hydrophilic and hydrophobic polyether sulfone (PES) membrane filtration performances. *Polymer Degradation and Stability, 168*, 108960.

Gonsalves, V. (1950). A critical investigation on the viscose filtration process. *Recueil des Travaux Chimiques des Pays-Bas, 69*(7), 873–903.

Grenier, A., Meireles, M., Aimar, P., & Carvin, P. (2008). Analysing flux decline in dead-end filtration. *Chemical Engineering Research and Design, 86*(11), 1281–1293.

Habib, M., Habib, U., Memon, A. R., Amin, U., Karim, Z., Khan, A. U., ... Ali, S. (2013). Predicting colloidal fouling of tap water by silt density index (SDI): Pore blocking in a membrane process. *Journal of Environmental Chemical Engineering, 1*(1–2), 33–37.

Hermia, J. (1982). Constant pressure blocking filtration laws-application to power-law non-Newtonian fluids. *Chemical Engineering Research and Design, 60*, 183–187.

Hwang, K.-J., & Lin, T.-T. (2002). Effect of morphology of polymeric membrane on the performance of cross-flow microfiltration. *Journal of Membrane Science, 199*(1–2), 41–52.

Jin, Y., Hengl, N., Baup, S., Pignon, F., Gondrexon, N., Magnin, A., ... Cabane, B. (2014). Effects of ultrasound on colloidal organization at nanometer length scale during cross-flow ultrafiltration probed by in-situ SAXS. *Journal of Membrane Science, 453*, 624–635.

Juang, R.-S., & Lin, K.-H. (2004). Flux recovery in the ultrafiltration of suspended solutions with ultrasound. *Journal of Membrane Science, 243*(1–2), 115–124.

Kailaku, S. I., Setiawan, B., & Sulaeman, A. (2017). The shelf life estimation of cold sterilized coconut water. *PLANTA TROPIKA: Jurnal Agrosains (Journal of Agro Science), 5*(1), 62–69.

Karmakar, S., & De, S. (2017). Cold sterilization and process modeling of tender coconut water by hollow fibers. *Journal of Food Engineering, 200*, 70–80.

Lamminen, M. O., Walker, H. W., & Weavers, L. K. (2004). Mechanisms and factors influencing the ultrasonic cleaning of particle-fouled ceramic membranes. *Journal of Membrane Science, 237*(1–2), 213–223.

Latt, K. K., & Kobayashi, T. (2006). Ultrasound-membrane hybrid processes for enhancement of filtration properties. *Ultrasonics Sonochemistry, 13*(4), 321–328.

Magalhães, M. P., Gomes, F., Modesta, R. C. D., Matta, V. M., & Cabral, L. M. C. (2005). Conservation of green cococnut water by membrane filtration. *Food Science and Technology, 25*(1), 72–77.

Mahnot, N. K., Kalita, D., Mahanta, C. L., & Chaudhuri, M. K. (2014). Effect of additives on the quality of tender coconut water processed by nonthermal two stage microfiltration technique. *LWT-Food Science and Technology, 59*(2), 1191–1195.

Maruyama, T., Katoh, S., Nakajima, M., & Nabetani, H. (2001). Mechanism of bovine serum albumin aggregation during ultrafiltration. *Biotechnology and Bioengineering, 75*(2), 233–238.

Matsui, K. N., Gut, J. A. W., De Oliveira, P. V., & Tadini, C. C. (2008). Inactivation kinetics of polyphenol oxidase and peroxidase in green coconut water by microwave processing. *Journal of Food Engineering, 88*(2), 169–176.

Mittal, R., Tavanandi, H. A., Mantri, V. A., & Raghavarao, K. (2017). Ultrasound assisted methods for enhanced extraction of Phycobiliproteins from marine macro-algae, Gelidium pusillum (Rhodophyta). *Ultrasonics Sonochemistry, 38*, 92–103.

Muthukumaran, S., Yang, K., Seuren, A., Kentish, S., Ashokkumar, M., Stevens, G. W., & Grieser, F. (2004). The use of ultrasonic cleaning for ultrafiltration membranes in the dairy industry. *Separation and Purification Technology, 39*(1–2), 99–107.

Narayan, A., Nagaraj, N., Hebbar, H. U., Chakkaravarthi, A., Raghavarao, K., & Nene, S. (2002). Acoustic field-assisted osmotic membrane distillation. *Desalination, 147*(1–3), 149–156.

Nielsen, S. S. (2010). Phenol-sulfuric acid method for total carbohydrates. *Food analysis laboratory manual* (pp. 47–53). Springer.

Nourbakhsh, H., Emam-Djomeh, Z., Mirsaeedghazi, H., Omid, M., & Moieni, S. (2014). Study of different fouling mechanisms during membrane clarification of red plum juice. *International Journal of Food Science & Technology, 49*(1), 58–64.

Palacio, L., Ho, C. C., & Zydney, A. L. (2002). Application of a pore-blockage—Cake-filtration model to protein fouling during microfiltration. *Biotechnology and Bioengineering, 79*(3), 260–270.

Prades, A., Dornier, M., Diop, N., & Pain, J.-P. (2012). Coconut water uses, composition and properties: A review. *Fruits, 67*(2), 87–107.

Purkayastha, M. D., Kalita, D., Das, V. K., Mahanta, C. L., Thakur, A. J., & Chaudhuri, M. K. (2012). Effects of L-ascorbic acid addition on micro-filtered coconut water: Preliminary quality prediction study using 1H-NMR, FTIR and GC-MS. *Innovative Food Science & Emerging Technologies, 13*, 184–199.

Ranganna, S. (1986). *Handbook of analysis and quality control for fruit and vegetable products.* Tata McGraw-Hill Education.

Reddy, K., Das, M., & Das, S. (2005). Filtration resistances in non-thermal sterilization of green coconut water. *Journal of Food Engineering, 69*(3), 381–385.

Reddy, K. V., Das, M., & Das, S. K. (2007). Nonthermal sterilization of green coconut water for packaging. *Journal of Food Quality, 30*(4), 466–480.

Saha, N., Balakrishnan, M., & Ulbricht, M. (2009). Fouling control in sugarcane juice ultrafiltration with surface modified polysulfone and polyethersulfone membranes. *Desalination, 249*(3), 1124–1131.

Sarkar, B. (2013). A combined complete pore blocking and cake filtration model during ultrafiltration of polysaccharide in a batch cell. *Journal of Food Engineering, 116*(2), 333–343.

Simon, A., Penpenic, L., Gondrexon, N., Taha, S., & Dorange, G. (2000). A comparative study between classical stirred and ultrasonically-assisted dead-end ultrafiltration. *Ultrasonics Sonochemistry, 7*(4), 183–186.

Tan, T.-C., Cheng, L.-H., Bhat, R., Rusul, G., & Easa, A. M. (2014). Composition, physicochemical properties and thermal inactivation kinetics of polyphenol oxidase and peroxidase from coconut (Cocos nucifera) water obtained from immature, mature and overly-mature coconut. *Food Chemistry, 142*, 121–128.

Thapa, N., Pal, J., & Tamang, J. P. (2004). Microbial diversity in ngari, hentak and tungtap, fermented fish products of North-East India. *World Journal of Microbiology and Biotechnology, 20*(6), 599.

Vigliar, R., Sdepanian, V. L., & Fagundes-Neto, U. (2006). Biochemical profile of coconut water from coconut palms planted in an inland region. *Jornal de Pediatria, 82*(4), 308–312.

Wang, L., Wang, X., & Fukushi, K. (2008). Effects of operational conditions on ultrafiltration membrane fouling. *Desalination, 229*(1–3), 181–191.

Yong, J. W., Ge, L., Ng, Y. F., & Tan, S. N. (2009). The chemical composition and biological properties of coconut (Cocos nucifera L.) water. *Molecules, 14*(12), 5144–5164.